mathematics

Article

Hierarchical Quantum Information Splitting of an Arbitrary Two-Qubit State Based on a Decision Tree

Dongfen Li *, Yundan Zheng, Xiaofang Liu, Jie Zhou, Yuqiao Tan, Xiaolong Yang and Mingzhe Liu

School of Computer and Network Security, Chengdu University of Technology, Chengdu 610059, China
* Correspondence: lidongfen17@cdut.edu.cn

Abstract: Quantum informatics is a new subject formed by the intersection of quantum mechanics and informatics. Quantum communication is a new way to transmit quantum states through quantum entanglement, quantum teleportation, and quantum information splitting. Based on the research of multiparticle state quantum information splitting, this paper innovatively combines the decision tree algorithm of machine learning with quantum communication to solve the problem of channel particle allocation in quantum communication, and experiments showed that the algorithm can make the optimal allocation scheme. Based on this scheme, we propose a two-particle state hierarchical quantum information splitting scheme based on the multi-particle state. First, Alice measures the Bell states of the particles she owns and tells the result to the receiver through the classical channel. If the receiver is a high-level communicator, he only needs the help of one of the low-level communicators and all the high-level communicators. After performing a single particle measurement on the z-basis, they send the result to the receiver through the classical channel. When the receiver is a low-level communicator, all communicators need to measure the particles they own and tell the receiver the results. Finally, the receiver performs the corresponding unitary operation according to the received results. In this regard, a complete hierarchical quantum information splitting operation is completed. On the basis of theoretical research, we also carried out experimental verification, security analysis, and comparative analysis, which shows that our scheme is reliable and has high security and efficiency.

Keywords: quantum communication; hierarchical quantum information splitting; digital technology; machine learning; decision tree

MSC: 68T20

check for updates

Citation: Li, D.; Zheng, Y.; Liu, X.; Zhou, J.; Tan, Y.; Yang, X.; Liu, M. Hierarchical Quantum Information Splitting of an Arbitrary Two-Qubit State Based on a Decision Tree. *Mathematics* **2022**, *10*, 4571. https://doi.org/10.3390/math10234571

Academic Editors: Shuo Yu, Feng Xia, Ignazio Licata and Ioannis G. Tsoulos

Received: 11 October 2022
Accepted: 28 November 2022
Published: 2 December 2022

1. Introduction

Quantum informatics is a new subject formed by the intersection of quantum mechanics and informatics. Quantum communication is a new form of communication. Its characteristic is to use the methods of quantum physics to transmit information safely and efficiently. As early as 1999, Hillery et al. [1] proposed the idea of quantum information splitting. After that, Murao, grudka et al. [2–16] improved the hierarchical quantum information splitting scheme by changing the particle state of the quantum information splitting channel, assigning different rights to communicators and expanding the hierarchical quantum information splitting scheme to probabilistic hierarchical quantum information splitting. It is worth noting that after 20 years of development, quantum information splitting has gradually moved from theory to reality. Literature [17–21] describes various experiments of quantum communication, such as the cavity QED experiment, ion trap experiment, and quantum critical distribution protocol experiment on an 80 km optical fiber, which was the first step to realizing the combination of quantum communication and digital technology. In 2020, Zhang et al. [22] proposed using artificial neural networks to quantify the controllability of quantum states, revealing the practical application of machine learning methods in exploring quantum steering. In the same year, wallnöfer et al. [23] proposed using machine learning to deal with environmental factors, making the quantum state more stable and improving the fidelity of communication. In 2021, lamata [24] proposed to use reinforcement learning to strengthen quantum communication and improve communication efficiency. The authors of [25,26] improved the existing quantum key distribution scheme. This scheme, combining machine learning and quantum key distribution, improves the transmission efficiency, but the current scheme still has problems, such as resource constraints, low efficiency, and poor information security. In 2020, Bebrov et al. [27] proposed the concept of quantum channel compression, which saves on the use of resources used in quantum secure-communication protocols. In 2021, verma [28] proposed an asymmetric two-way quantum teleportation protocol based on local CNOT gate operation. Compared with previous two-way quantum teleportation protocols, this protocol consumes less quantum and classical resources and has higher internal efficiency and less operational complexity. In the same year, Feng et al. [29] proposed a quantum dialogue protocol based on identity authentication, reducing quantum resource consumption by combining identity authentication with channel security detection. In 2022, Choudhury et al. [30] proposed a tripartite quantum conference scheme which solved the problem of exchanging information between multiple communicators and opened up a new research direction.

Based on the research of the above scheme and the relevant discussion of the decision tree algorithm in machine learning in literature [31–36], we innovatively combined machine learning with quantum communication technology and uses decision tree algorithm to optimize resource allocation and improve transmission efficiency. A hierarchical quantum information splitting of an arbitrary two-qubit state based on decision tree (HQSD) is proposed.

The rest of this paper consists of the following parts. Section 2 describes the process for the overall design of the scheme step by step. In Section 3, the process of the decision tree making the optimal allocation model of information particles is described. In Section 4, the quantum information splitting scheme based on eight particle-cluster states is described in detail, and the quantum channel is extended to multi-particle states. Section 5 is the experimental verification and analysis of the scheme. Sections 6 and 7 summarize the full text and present prospects.

2. Overall Design of the Scheme

In this paper, to solve the problem of channel particle allocation for communicators in practical applications, we first use the decision tree algorithm and MATLAB to design experiments, which show that the decision tree algorithm can indeed solve the problem of channel particle allocation for communicators, and to determine the best allocation scheme. Then, we propose a hierarchical quantum information splitting scheme based on eight-qubit state. The hierarchical rules based on multi-particle states are summarized, and then the scheme is verified by experiments, proving the scheme's feasibility. Finally, the security analysis and comparative analysis are presented, and it is concluded that the scheme has the characteristics of safety, effectiveness, and low energy consumption.

The overall frame diagram is shown in Figure 1, and the specific steps are as follows:

(1) First, use the decision tree algorithm to make the optimal communication decision for channel particle allocation.
(2) Then, we assume that Alice is the sender; and the communication participants are Bob1, Bob2, Charlie1, Charlie2, and Charlie3. According to the decision, Bob1 and Bob2 are high-level communicators, and Charlie1, Charlie2, and Charlie3 are low-level communicators. Different receivers have different particle distribution schemes.
(3) Next, Alice conducts Bell-state measurement on the particle pair (A, 1), (B, 2). When the receiver is a high-level communicator, only one of Bob2 and a low-level communicator is required to perform a Z-based single particle measurement; after the measurement operation is performed, the result is reported to the receiver through the classical channel. When the receiver is a low-level communicator, all communication

participants need to perform the measurement, and the low-level communicator needs to perform X-based single-particle measurements. Then, the communicator sends the result to the receiver.

(4) Finally, after receiving all the measurement results, the receiver conducts a unitary operation on the collapsed state using the corresponding results. It can recover any two-qubit state information that Alice intends to send.

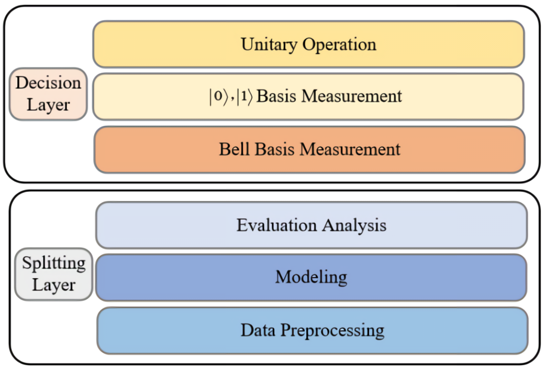

Figure 1. Overall framework.

3. An Optimal Allocation Model of Channel Particles Based on a Decision Tree

In the scheme, we need to evaluate the levels of the communication participants and then assign the corresponding particle to the communicator according to its level. Since the number of people involved in communication may be quite large, the conditions for judging the level are too complicated, etc., it is difficult for us to evaluate the level of the communicator. Therefore, the decision tree algorithm can be adapted to solving the problem of hierarchical quantum information splitting channel particle allocation, and we can use another algorithm to decide on the best solution. In order to solve the problem of channel particle allocation, it is actually necessary to solve the problem of judging the levels of communicators. We should divide the communication participants into two categories, high-level communicators and low-level communicators. The decision tree can learn to generate a decision model that can deal with unknown examples according to the existing classification rules. We use this feature to make optimal decisions and used the existing decision tree function in MATLAB to design the model.

3.1. Data Preprocessing

We have set up four main factors for evaluating the levels of correspondents. These factors are also the characteristics of the data. They are the proportion of honesty in all communications, the number of honest communications in the last three communications, and the dishonesty judged by the third-party notary platform and availability. Among them, honesty means that the communicator will not interfere with the regular communication in the communication process; that is, the communicator will not communicate as the eavesdropper. Then, in order to facilitate the learning of the decision tree algorithm, all the data were represented by numbers. We evaluated whether the communicator is honest according to the characteristics and use numbers to express it. Finally, the total sample size of all the collected data was 1131, and the data were organized into the proportions greater than or equal to 0.5 and less than 0.5. The probability of being honest was 0. There were 409 high-level correspondents and 722 low-level correspondents. These are model 1's data.

3.2. Model Establishment and Evaluation Analysis

First, the decision tree will generate a decision model after learning the dataset, and then to avoid loss of generality, to avoid the phenomenon of overfitting, we need to optimize the generated decision model. The commonly used method is to limit or prune the decision model according to cross-validation results. In order to make the generated decision model not limited to one dataset, we introduce a resampling error. We calculated the cross-validation error and resampling error of the decision model before and after optimization, and compared and analyze whether the decision model reached the expectation. In addition, to avoid contingency, we reorganized the data and divided the levels of correspondents according to the participating in all communications or not, the proportion of honest communication and the possibility of dishonesty judged by the third-party notary platform. Correspondents with a ratio greater than or equal to 0.5 and a probability of dishonesty of 0 were considered high-level. Compared with the previously compiled data, the prominence of the feature of listing or not was reduced, and the proportion of the feature of the number of times of honesty in the last three communications was considered. The sample was 1131, with 689 for the low and 442 for the high levels. Finally, we repeatedly checked the model by evaluation and analysis, classified all experimental data, and evaluated them separately to evaluate the capability of decision model and whether the decision plan is reliable and efficient.

3.3. Optimal Allocation Model of Channel Particles

According to the previous content, we first designed model 1, as shown in Figure 2. In Figure 2, $\times 1$ is the proportion of the number of occasions of honesty among all communications, $\times 3$ is the possibility of being dishonesty judged by the third-party notary platform, $\times 4$ is whether to go public; the classification standard of its tree structure and our pre-established classification standard are the same. The generated decision model no longer needs to be pruned. It achieved the desired effect and can be well adapted to the new dataset from the performance test results. There will be no over-fitting phenomenon, so we only need to restrict the decision model, and the result is shown in Figure 3.

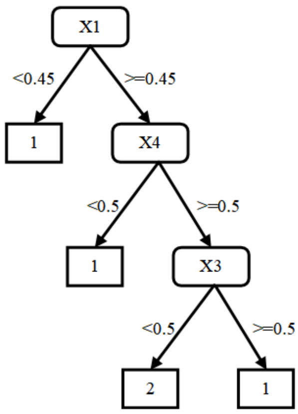

Figure 2. Model 1.

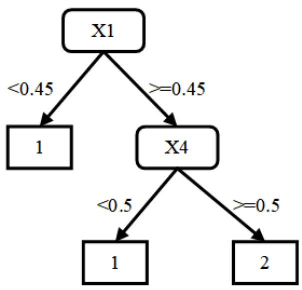

Figure 3. Model 1(a) limiting the number of leaf node samples.

In terms of the resampling error combined with the cross-validation error, the restricted decision model slightly increases the error value compared to the previous one.As shown in Table 1.

Table 1. Decision model resampling error and cross-validation error values.

Model	Resampling Error	Cross-Validation Error
Model 1	0	0
Model 1(a)	0.002	0.002

For model 2, similarly, we first train and then test. After the algorithm learns, it will generate the decision model, as evinced in Figure 4. Compared with the decision model in model 1, the decision model is more complex, indicating that the classification rules of the decision model changed after data sorting. We can see the ×2 feature, that is, the number of honest messages in the last three communications, reflected in the tree structure, to achieve the expected effect we want, and after modeling many times, the decision tree continues to learn and the accuracy continues to improve and approaches 100%. We can conclude that under ideal conditions, it can eventually be improved to 100%, proving the decision tree algorithm can decide on the optimal solution. The results are evinced in Figure 5.

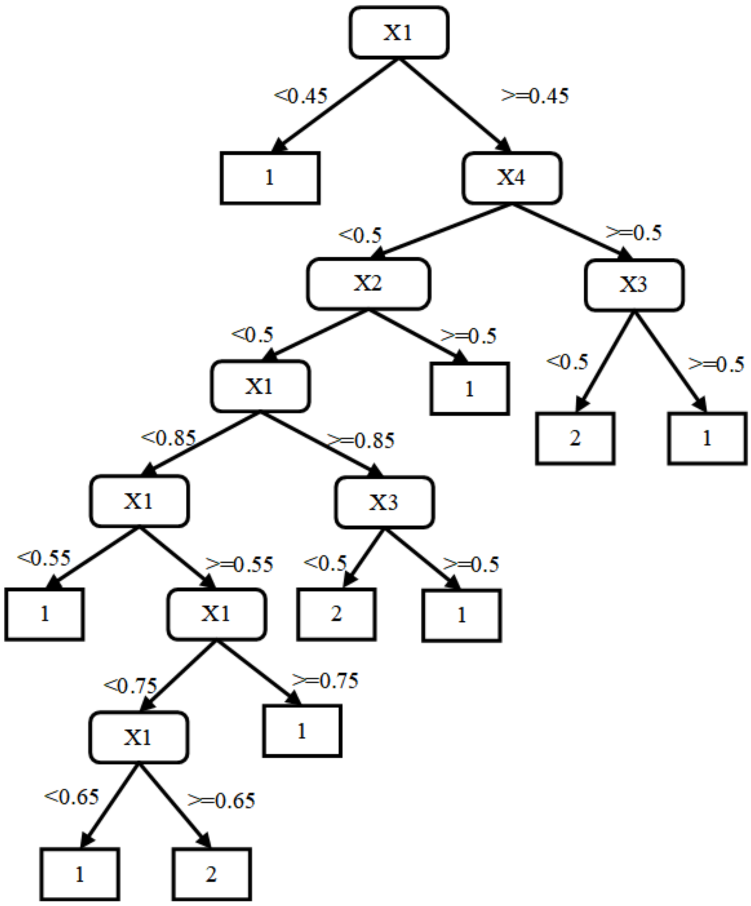

Figure 4. Model 2.

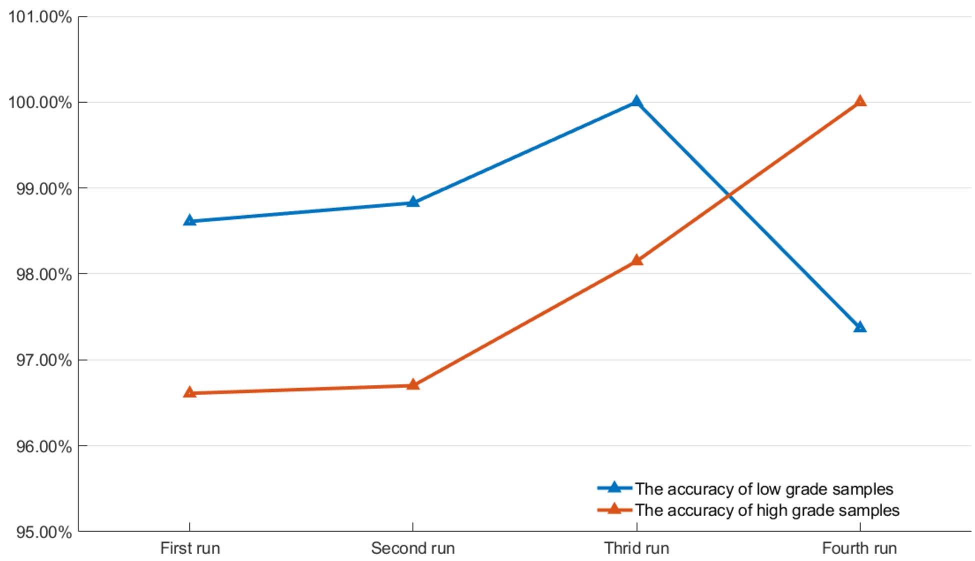

Figure 5. Test set sample accuracy.

Next, the capability of the decision model was evaluated, and the method of setting the minimum number of samples and pruning was used to enhance the generalization ability of the decision model and avoid overfitting. First, the influence of the number of samples on the performance of the decision model was calculated. After the cross-validation error succeeded in diminishing with the increase of the number of samples, after reaching the lowest point, it began to increase. According to the principle of minimum parameters, a model with a cross-validation error value of 0.015 was selected, and its resampling error was calculated, as evinced in Figure 6.

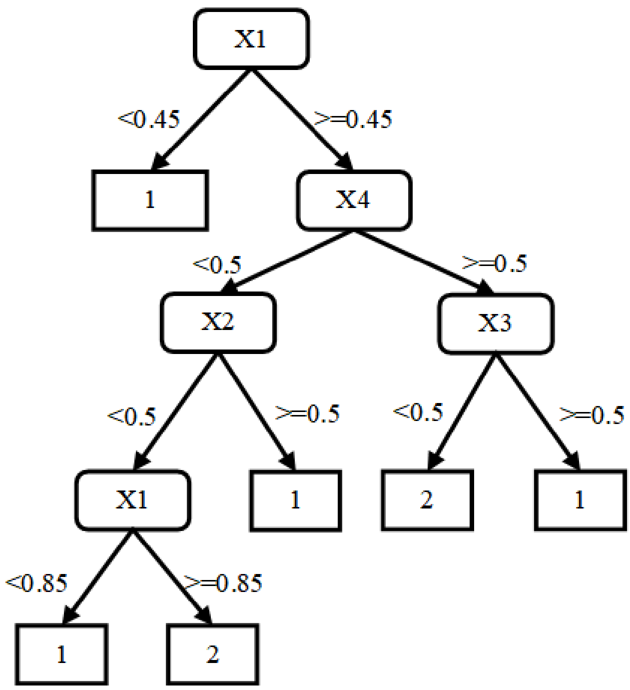

Figure 6. Decision tree model 2(b) with minimum cross-validation error.

Then, using the pruning method, we also found that the pruning result is 0, and no pruning is needed. We calculated the resampling and cross-validation errors and compared them with mode 2 and the decision tree with the minimum number of sample leaf nodes at the beginning, model 2(a). The results of the decision model calculation of the number of leaf nodes are compared; see Table 2. From the comparison of the resampling results and cross-validation errors of the three decision models, the resampling error value and cross-validation error value of model 2(a) are larger than those of the original decision model, but the difference is minimal.

Table 2. The resampling error and cross-validation error values of decision model 2.

Model	Resampling Error	Cross-Validation Error
Model 2	0.007	0.009
Model 2(a)	0.015	0.015
Model 2(b)	0.007	0.01

Without changing the dataset, we kept running and repeating modeling, and the accuracy rate was constantly improving. Model 3 had an accuracy rate of 98.6301% for low-level samples and a rate of 100% for high-level samples, as shown in Figure 7a. Compare it with Figure 3; there is no difference in the tree structure. However, the classification value of the node changed. Similarly, we also optimized it. After calculating the cross-validation error, the number of leaf nodes in the decision model was 16. For the cross-validation error value of 0.02, which is the minimum value, the decision model is evinced in Figure 7b. The pruned decision model is evinced in Figure 7c. The pruning result is one, indicating that the first layer of the original decision model has been pruned. The resampling error values and cross-validation error values of the above three decision models are shown in Table 3.

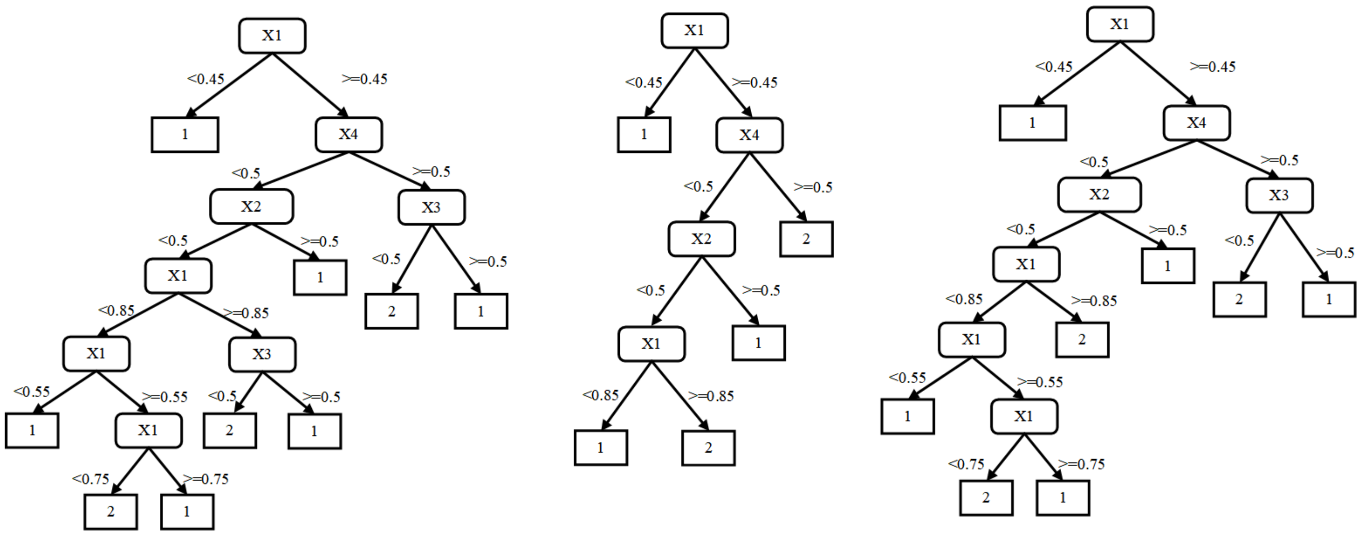

(**a**) (**b**) (**c**)

Figure 7. Model 3. From left to right are (**a**) the generated decision model, (**b**) the decision model with the least value for the leaf node, (**c**) the decision model after pruning.

Table 3. The resampling error and cross-validation error values of decision model 3.

Model	Resampling Error	Cross-Validation Error
Model 3(a)	0.009	0.015
Model 3(b)	0.018	0.021
Model 3(c)	0.01	0.016

Comparing the results of model 2 and model 3, it is not the case that the higher the accuracy, the better the performance of the decision model. Furthermore, comparing the pruned decision model and the decision model with the lowest number of leaf nodes, it is evident that the tree structure of the decision model with the fewest leaf nodes is simpler.

However, the error values are relatively large. It cannot be ruled out that the optimized decision model is more suitable for application due to the limitation of the set dataset. According to all the evaluations obtained for the model, there are specific errors in the results due to the limitations of the dataset and the existence of certain influencing factors in the simulation. However, these error values are minimal and negligible. We can conclude that the decision tree algorithm can solve the channel problem. Moreover, the algorithm achieved the set goal in our preset dataset, which verifies that the decision tree algorithm can decide on the optimal allocation scheme. The generated model has good generalization ability and can adapt to a more completely random dataset environment; that is, it works better in practice.

4. Hierarchical Quantum Information Splitting Scheme for Arbitrary Two-Qubit State Based on Multi-Qubit State

After obtaining the best plan according to the above, according to the assigned strategy, in the specific hierarchical quantum information splitting plan, we assume that there are five participants, namely Alice, Bob1, Bob2, Charlie1, Charlie2, and Charlie3. Among them, Alice is the sender, and the information to be sent is any two-qubit state $|\psi\rangle_{AB} = \frac{1}{2}(\alpha|00\rangle + \beta|01\rangle + \gamma|10\rangle + \sigma|11\rangle)_{AB}$. Here, $\alpha, \beta, \gamma, \sigma$ are coefficients, which are in complex form and satisfy $|\alpha|^2 + |\beta|^2 + |\gamma|^2 + |\sigma|^2 = 1$. Correspondents Bob1 and Bob2 are seniors; and Charlie1, Charlie2, and Charlie3 are low-level communicators. They share an eight-qubit cluster state channel, as in Equation (1).

$$
\begin{aligned}
|\phi\rangle_{12345678} =& \frac{1}{2}(|00000000\rangle + |00000111\rangle + |00001000\rangle \\
&+ |00001111\rangle + |01010000\rangle + |01010111\rangle \\
&+ |01011000\rangle + |01011111\rangle + |10100000\rangle \\
&- |10100111\rangle + |10101000\rangle - |10101111\rangle \\
&+ |11110000\rangle - |11110111\rangle + |11111000\rangle \\
&- |11111111\rangle)_{12345678}
\end{aligned} \tag{1}
$$

In addition to any two-qubit state $|\psi\rangle_{AB}$, Alice also has particle 1 and particle 2 of the channel particle; and the receiver of information has particle 3 and particle 4. Other communication participants have only one particle. Before communicating, we rewrite the channel particle as follows:

$$
\begin{aligned}
|\phi\rangle_{12345678} = \frac{1}{\sqrt{2}}[&|00\rangle(|\psi^0\rangle + |\psi^1\rangle) + |01\rangle(|\psi^2\rangle + |\psi^3\rangle) \\
&+ |10\rangle(|\psi^4\rangle + |\psi^5\rangle) + |11\rangle(|\psi^6\rangle + |\psi^7\rangle)]_{12345678}
\end{aligned} \tag{2}
$$

$$
\begin{aligned}
|\psi^0\rangle &= \frac{1}{\sqrt{2}}|000\rangle(|000\rangle + |111\rangle) \quad & |\psi^1\rangle &= \frac{1}{\sqrt{2}}|001\rangle(|000\rangle + |111\rangle) \\
|\psi^2\rangle &= \frac{1}{\sqrt{2}}|010\rangle(|000\rangle + |111\rangle) \quad & |\psi^3\rangle &= \frac{1}{\sqrt{2}}|011\rangle(|000\rangle + |111\rangle) \\
|\psi^4\rangle &= \frac{1}{\sqrt{2}}|100\rangle(|000\rangle - |111\rangle) \quad & |\psi^5\rangle &= \frac{1}{\sqrt{2}}|101\rangle(|000\rangle - |111\rangle) \\
|\psi^6\rangle &= \frac{1}{\sqrt{2}}|110\rangle(|000\rangle - |111\rangle) \quad & |\psi^7\rangle &= \frac{1}{\sqrt{2}}|111\rangle(|000\rangle - |111\rangle)
\end{aligned} \tag{3}
$$

The original system state of the entire system can be described as:

$$
\begin{aligned}
|\psi\rangle = |\phi\rangle_{AB} \otimes |\phi\rangle_{12345678} = \frac{1}{2\sqrt{2}}[\alpha|0000\rangle(|\psi^0\rangle + |\psi^1\rangle) \\
+ \alpha|0001\rangle(|\psi^2\rangle + |\psi^3\rangle) + \alpha|0010\rangle(|\psi^4\rangle + |\psi^5\rangle) \\
+ \alpha|0011\rangle(|\psi^6\rangle + |\psi^7\rangle) + \beta|0100\rangle(|\psi^0\rangle + |\psi^1\rangle) \\
+ \beta|0101\rangle(|\psi^2\rangle + |\psi^3\rangle) + \beta|0110\rangle(|\psi^4\rangle + |\psi^5\rangle) \\
+ \beta|0111\rangle(|\psi^6\rangle + |\psi^7\rangle) + \gamma|1000\rangle(|\psi^0\rangle + |\psi^1\rangle) \\
+ \gamma|1001\rangle(|\psi^2\rangle + |\psi^3\rangle) + \gamma|1010\rangle(|\psi^4\rangle + |\psi^5\rangle) \\
+ \gamma|1011\rangle(|\psi^6\rangle + |\psi^7\rangle) + \sigma|1100\rangle(|\psi^0\rangle + |\psi^1\rangle) \\
+ \sigma|1101\rangle(|\psi^2\rangle + |\psi^3\rangle) + \sigma|1110\rangle(|\psi^4\rangle + |\psi^5\rangle) \\
+ \sigma|1111\rangle(|\psi^6\rangle + |\psi^7\rangle)]_{AB12345678}
\end{aligned} \tag{4}
$$

In order to realize the hierarchical quantum information splitting of a two-qubit state, Alice first operates Bell-state measurement on the particle pair (A, 1), (B, 2). After the measurement, other particles will collapse into one of 16 states. Each probability is equal, and Alice's measurement results and the collapsed state of the rest particles are shown in Table 4. The Bell-state measurement expression is as follows:

$$|\psi\rangle = \frac{1}{\sqrt{2}}(|00\rangle \pm |11\rangle) \quad |\phi\rangle = \frac{1}{\sqrt{2}}(|01\rangle \pm |10\rangle) \tag{5}$$

As the scheme is a hierarchical quantum information splitting scheme, the communication participants are divided into high-level and low-level. Next, we describe the process of reconstructing any two-qubit state when the receivers of different levels communicate.

Table 4. Collapse of the remaining particles after Alice performed the measurement.

The Measurement of Alice	The Collapse State after Measurement
$\|\psi\rangle^+\|\psi\rangle^+$	$\|\Psi^1\rangle_{345678} = \frac{1}{4\sqrt{2}}[\alpha(\|\psi^0\rangle + \|\psi^1\rangle) + \beta(\|\psi^2\rangle + \|\psi^3\rangle) + \gamma(\|\psi^4\rangle + \|\psi^5\rangle) + \sigma(\|\psi^6\rangle + \|\psi^7\rangle)]$
$\|\psi\rangle^+\|\psi\rangle^-$	$\|\Psi^2\rangle_{345678} = \frac{1}{4\sqrt{2}}[\alpha(\|\psi^0\rangle + \|\psi^1\rangle) - \beta(\|\psi^2\rangle + \|\psi^3\rangle) + \gamma(\|\psi^4\rangle + \|\psi^5\rangle) - \sigma(\|\psi^6\rangle + \|\psi^7\rangle)]$
$\|\psi\rangle^+\|\phi\rangle^+$	$\|\Psi^3\rangle_{345678} = \frac{1}{4\sqrt{2}}[\alpha(\|\psi^2\rangle + \|\psi^3\rangle) + \beta(\|\psi^0\rangle + \|\psi^1\rangle) + \gamma(\|\psi^6\rangle + \|\psi^7\rangle) + \sigma(\|\psi^4\rangle + \|\psi^5\rangle)]$
$\|\psi\rangle^+\|\phi\rangle^-$	$\|\Psi^4\rangle_{345678} = \frac{1}{4\sqrt{2}}[\alpha(\|\psi^2\rangle + \|\psi^3\rangle) - \beta(\|\psi^0\rangle + \|\psi^1\rangle) + \gamma(\|\psi^6\rangle + \|\psi^7\rangle) - \sigma(\|\psi^4\rangle + \|\psi^5\rangle)]$
$\|\psi\rangle^-\|\psi\rangle^+$	$\|\Psi^5\rangle_{345678} = \frac{1}{4\sqrt{2}}[\alpha(\|\psi^0\rangle + \|\psi^1\rangle) + \beta(\|\psi^2\rangle + \|\psi^3\rangle) - \gamma(\|\psi^4\rangle + \|\psi^5\rangle) - \sigma(\|\psi^6\rangle + \|\psi^7\rangle)]$
$\|\psi\rangle^-\|\psi\rangle^-$	$\|\Psi^6\rangle_{345678} = \frac{1}{4\sqrt{2}}[\alpha(\|\psi^0\rangle + \|\psi^1\rangle) - \beta(\|\psi^2\rangle + \|\psi^3\rangle) - \gamma(\|\psi^4\rangle + \|\psi^5\rangle) + \sigma(\|\psi^6\rangle + \|\psi^7\rangle)]$
$\|\psi\rangle^-\|\phi\rangle^+$	$\|\Psi^7\rangle_{345678} = \frac{1}{4\sqrt{2}}[\alpha(\|\psi^2\rangle + \|\psi^3\rangle) - \beta(\|\psi^0\rangle + \|\psi^1\rangle) - \gamma(\|\psi^6\rangle + \|\psi^7\rangle) + \sigma(\|\psi^4\rangle + \|\psi^5\rangle)]$
$\|\psi\rangle^-\|\phi\rangle^-$	$\|\Psi^8\rangle_{345678} = \frac{1}{4\sqrt{2}}[\alpha(\|\psi^2\rangle + \|\psi^3\rangle) - \beta(\|\psi^0\rangle + \|\psi^1\rangle) - \gamma(\|\psi^6\rangle + \|\psi^7\rangle) + \sigma(\|\psi^4\rangle + \|\psi^5\rangle)]$
$\|\phi\rangle^+\|\psi\rangle^+$	$\|\Psi^9\rangle_{345678} = \frac{1}{4\sqrt{2}}[\alpha(\|\psi^4\rangle + \|\psi^5\rangle) + \beta(\|\psi^6\rangle + \|\psi^7\rangle) + \gamma(\|\psi^0\rangle + \|\psi^1\rangle) + \sigma(\|\psi^2\rangle + \|\psi^3\rangle)]$
$\|\phi\rangle^+\|\psi\rangle^-$	$\|\Psi^{10}\rangle_{345678} = \frac{1}{4\sqrt{2}}[\alpha(\|\psi^4\rangle + \|\psi^5\rangle) - \beta(\|\psi^6\rangle + \|\psi^7\rangle) + \gamma(\|\psi^0\rangle + \|\psi^1\rangle) - \sigma(\|\psi^2\rangle + \|\psi^3\rangle)]$
$\|\phi\rangle^+\|\phi\rangle^+$	$\|\Psi^{11}\rangle_{345678} = \frac{1}{4\sqrt{2}}[\alpha(\|\psi^6\rangle + \|\psi^7\rangle) + \beta(\|\psi^4\rangle + \|\psi^5\rangle) + \gamma(\|\psi^2\rangle + \|\psi^3\rangle) + \sigma(\|\psi^0\rangle + \|\psi^1\rangle)]$
$\|\phi\rangle^+\|\phi\rangle^-$	$\|\Psi^{12}\rangle_{345678} = \frac{1}{4\sqrt{2}}[\alpha(\|\psi^6\rangle + \|\psi^7\rangle) - \beta(\|\psi^4\rangle + \|\psi^5\rangle) + \gamma(\|\psi^2\rangle + \|\psi^3\rangle) - \sigma(\|\psi^0\rangle + \|\psi^1\rangle)]$
$\|\phi\rangle^-\|\psi\rangle^+$	$\|\Psi^{13}\rangle_{345678} = \frac{1}{4\sqrt{2}}[\alpha(\|\psi^4\rangle + \|\psi^5\rangle) + \beta(\|\psi^6\rangle + \|\psi^7\rangle) - \gamma(\|\psi^0\rangle + \|\psi^1\rangle) - \sigma(\|\psi^2\rangle + \|\psi^3\rangle)]$
$\|\phi\rangle^-\|\psi\rangle^-$	$\|\Psi^{14}\rangle_{345678} = \frac{1}{4\sqrt{2}}[\alpha(\|\psi^4\rangle + \|\psi^5\rangle) - \beta(\|\psi^6\rangle + \|\psi^7\rangle) - \gamma(\|\psi^0\rangle + \|\psi^1\rangle) + \sigma(\|\psi^2\rangle + \|\psi^3\rangle)]$
$\|\phi\rangle^-\|\phi\rangle^+$	$\|\Psi^{15}\rangle_{345678} = \frac{1}{4\sqrt{2}}[\alpha(\|\psi^6\rangle + \|\psi^7\rangle) + \beta(\|\psi^4\rangle + \|\psi^5\rangle) - \gamma(\|\psi^2\rangle + \|\psi^3\rangle) - \sigma(\|\psi^0\rangle + \|\psi^1\rangle)]$
$\|\phi\rangle^-\|\phi\rangle^-$	$\|\Psi^{16}\rangle_{345678} = \frac{1}{4\sqrt{2}}[\alpha(\|\psi^6\rangle + \|\psi^7\rangle) - \beta(\|\psi^4\rangle + \|\psi^5\rangle) - \gamma(\|\psi^2\rangle + \|\psi^3\rangle) + \sigma(\|\psi^0\rangle + \|\psi^1\rangle)]$

4.1. Information Splitting When Receiver Authority Is High

Assuming that Bob1 is the receiver, he has particle 3 and particle 4; Bob2 has particle 5; and Charlie1, Charlie2, and Charlie3 have particle 6, particle 7, and particle 8, respectively. Let us illustrate with an example that when Alice's measurement is $|\psi\rangle^{+}|\phi\rangle^{+}$, other particles will collapse into

$$\begin{aligned}|\psi^1\rangle_{345678} =& \frac{1}{4\sqrt{2}}[\alpha(|\phi^0\rangle + |\phi^1\rangle) + \beta(|\phi^2\rangle + |\phi^3\rangle) \\ &+ \gamma(|\phi^4\rangle + |\phi^5\rangle) + \sigma(|\phi^6\rangle + |\phi^7\rangle)]_{345678} \\ =& \frac{1}{8}[(\alpha|00\rangle + \beta|01\rangle + \gamma|10\rangle + \sigma|11\rangle)|0\rangle|000\rangle \\ &+ (\alpha|00\rangle + \beta|01\rangle - \gamma|10\rangle - \sigma|11\rangle)|0\rangle|111\rangle \\ &+ (\alpha|00\rangle + \beta|01\rangle + \gamma|10\rangle + \sigma|11\rangle)|1\rangle|000\rangle \\ &+ (\alpha|00\rangle + \beta|01\rangle - \gamma|10\rangle - \sigma|11\rangle)|1\rangle|111\rangle]_{345678}\end{aligned} \tag{6}$$

Then Bob2, Charlie1, Charlie2, and Charlie3 perform Z-based single particle measurement, respectively, and tell Bob1 the results through the classical channel, and Bob1 can rebuild the original two-particle state by operating a unitary operation following the corresponding measurement result. We can find from Equation (6) that since the channel particle we constructed is symmetric, the results of Charlie1, Charlie2, and Charlie3 are always correlated. When the measurement result of one of them is known, the other communicators can be inferred, so we only need to perform Z-based single particle measurement on any of Charlie1, Charlie2, and Charlie3.

Therefore, when the receiver is high-level, we only need one low-level communicator to perform Z-based single particle measurement, and the measurement results of other communicators can be deduced from the obtained results. They are sent to the receiver. Due to the corresponding measurement result, the receiver operates the relevant unitary operation to reconstruct any two-qubit state sent by the sender. The relevant results are shown in Table 5. The four unitary operations are:

$$\begin{aligned}I &= I = |0\rangle\langle 0| + |1\rangle\langle 1| \\ \sigma_z &= Z = |0\rangle\langle 0| - |1\rangle\langle 1| \\ \sigma_x &= X = |0\rangle\langle 1| + |1\rangle\langle 0| \\ \mathrm{i}\sigma_y &= Y = |0\rangle\langle 1| - |1\rangle\langle 0|\end{aligned} \tag{7}$$

4.2. Information Splitting When Receiver Authority Is Low

We assume that Charlie1 is the receiver. Charlie1 will be assigned to have two particles, particle 3 and particle 4; Bob1 and Bob2 have particle 5 and particle 6, respectively; and Charlie2 and Charlie3 have particle 7 and particle 8, respectively. Similarly, we take Alice's measurement as an example to illustrate then the collapsed state of the rest particle is rewritten as

$$
\begin{aligned}
|\psi^1\rangle_{567834} =&[\frac{1}{16}|00\rangle(|++\rangle+|+-\rangle+|-+\rangle+|--\rangle)\\
&\otimes(\alpha|00\rangle+\beta|01\rangle+\gamma|10\rangle+\sigma|11\rangle)\\
&+\frac{1}{16}|01\rangle(|++\rangle-|+-\rangle-|-+\rangle+|--\rangle)\\
&\otimes(\alpha|00\rangle+\beta|01\rangle-\gamma|10\rangle-\sigma|11\rangle)\\
&+\frac{1}{16}|10\rangle(|++\rangle+|+-\rangle+|-+\rangle+|--\rangle)\\
&\otimes(\alpha|00\rangle+\beta|01\rangle+\gamma|10\rangle+\sigma|11\rangle)\\
&+\frac{1}{16}|11\rangle(|++\rangle-|+-\rangle-|-+\rangle+|--\rangle)\\
&\otimes(\alpha|00\rangle+\beta|01\rangle-\gamma|10\rangle-\sigma|11\rangle)]_{567834}
\end{aligned}
\tag{8}
$$

Among them, $|+\rangle = \frac{1}{\sqrt{2}}(|0\rangle + |1\rangle), |-\rangle = \frac{1}{\sqrt{2}}(|0\rangle - |1\rangle)$. From Equation (8), we can see that the results of Charlie2 and Charlie3 are not correlated with each other at this time, so when the low-level communicator receives a message, all the communicating participants need to perform measurements on the particles they own, the low-level communicator. The communicator ought to perform an X-based single particle measurement and inform Charlie1 of the result through the classical channel, and then Charlie1 can restore the original information through the corresponding unitary operation. The results are shown in Table 6.

Table 5. The measurement results after Bob2, Charlie1, Charlie2, and Charlie3 performing the measurement, the state obtained by Bob1 and the corresponding unitary operation.

Measurement Results of Bob2, Charlie1, Charlie2 and Charlie3 [1]	**The State Obtained by Bob1**	**Unitary Operation**
$(|0000\rangle,|1000\rangle)or(|0111\rangle,|1111\rangle)$	$\frac{1}{4}(\alpha|00\rangle+\beta|01\rangle+\gamma|10\rangle+\sigma|11\rangle)$	$I_3\otimes I_4$
$(|0111\rangle,|1111\rangle)or(|0000\rangle,|1000\rangle)$	$\frac{1}{4}(\alpha|00\rangle+\beta|01\rangle-\gamma|10\rangle-\sigma|11\rangle)$	$z_3\otimes I_4$
$(|0000\rangle,|1000\rangle)or(|0111\rangle,|1111\rangle)$	$\frac{1}{4}(\alpha|00\rangle-\beta|01\rangle+\gamma|10\rangle-\sigma|11\rangle)$	$I_3\otimes z_4$
$(|0111\rangle,|1111\rangle)or(|0000\rangle,|1000\rangle)$	$\frac{1}{4}(\alpha|00\rangle-\beta|01\rangle-\gamma|10\rangle+\sigma|11\rangle)$	$Z_3\otimes Z_4$
$(|0000\rangle,|1000\rangle)or(|0111\rangle,|1111\rangle)$	$\frac{1}{4}(\alpha|01\rangle+\beta|00\rangle+\gamma|11\rangle+\sigma|10\rangle)$	$I_3\otimes X_4$
$(|0111\rangle,|1111\rangle)or(|0000\rangle,|1000\rangle)$	$\frac{1}{4}(\alpha|01\rangle+\beta|00\rangle-\gamma|11\rangle-\sigma|10\rangle)$	$Z_3\otimes X_4$
$(|0000\rangle,|1000\rangle)or(|0111\rangle,|1111\rangle)$	$\frac{1}{4}(\alpha|01\rangle-\beta|00\rangle+\gamma|11\rangle-\sigma|10\rangle)$	$I_3\otimes X_4\otimes Z_4$
$(|0111\rangle,|1111\rangle)or(|0000\rangle,|1000\rangle)$	$\frac{1}{4}(\alpha|01\rangle-\beta|00\rangle-\gamma|11\rangle+\sigma|10\rangle)$	$Z_3\otimes Y_4$
$|0000\rangle,|1000\rangle$	$\frac{1}{4}(\alpha|10\rangle+\beta|11\rangle+\gamma|00\rangle+\sigma|01\rangle)$	$X_3\otimes I_4$
$|0111\rangle,|1111\rangle$	$\frac{1}{4}(-\alpha|10\rangle-\beta|11\rangle+\gamma|00\rangle+\sigma|01\rangle)$	$z_3\otimes X_3\otimes I_4$
$|0000\rangle,|1000\rangle$	$\frac{1}{4}(\alpha|10\rangle-\beta|11\rangle+\gamma|00\rangle-\sigma|01\rangle)$	$X_3\otimes Z_4$
$|0111\rangle,|1111\rangle$	$\frac{1}{4}(-\alpha|10\rangle+\beta|11\rangle+\gamma|00\rangle-\sigma|01\rangle)$	$Z_3\otimes X_3\otimes Z_4$
$|0000\rangle,|1000\rangle$	$\frac{1}{4}(\alpha|10\rangle+\beta|11\rangle-\gamma|00\rangle-\sigma|01\rangle)$	$Z_3\otimes X_3\otimes I_4$
$|0111\rangle,|1111\rangle$	$\frac{1}{4}(-\alpha|10\rangle-\beta|11\rangle-\gamma|00\rangle-\sigma|01\rangle)$	$Z_3\otimes X_3\otimes Z_3\otimes I_4$
$|0000\rangle,|1000\rangle$	$\frac{1}{4}(\alpha|10\rangle-\beta|11\rangle-\gamma|00\rangle+\sigma|01\rangle)$	$Y_3\otimes Z_4$
$|0111\rangle,|1111\rangle$	$\frac{1}{4}(-\alpha|10\rangle+\beta|11\rangle-\gamma|00\rangle+\sigma|01\rangle)$	$Z_3\otimes X_3\otimes Z_3\otimes Z_4$
$|0000\rangle,|1000\rangle$	$\frac{1}{4}(\alpha|11\rangle+\beta|10\rangle+\gamma|01\rangle+\sigma|00\rangle)$	$X_3\otimes X_4$
$|0111\rangle,|1111\rangle$	$\frac{1}{4}(-\alpha|11\rangle-\beta|10\rangle+\gamma|01\rangle+\sigma|00\rangle)$	$Z_3\otimes X_3\otimes X_4$
$|0000\rangle,|1000\rangle$	$\frac{1}{4}(\alpha|11\rangle-\beta|10\rangle+\gamma|01\rangle-\sigma|00\rangle)$	$X_3\otimes X_4\otimes Z_4$
$|0111\rangle,|1111\rangle$	$\frac{1}{4}(-\alpha|11\rangle+\beta|10\rangle+\gamma|01\rangle-\sigma|00\rangle)$	$Z_3\otimes X_3\otimes X_4\otimes Z_4$
$|0000\rangle,|1000\rangle$	$\frac{1}{4}(\alpha|11\rangle+\beta|10\rangle-\gamma|01\rangle-\sigma|00\rangle)$	$X_3\otimes X_4\otimes Z_3$
$|0111\rangle,|1111\rangle$	$\frac{1}{4}(-\alpha|11\rangle-\beta|10\rangle-\gamma|01\rangle-\sigma|00\rangle)$	$Z_3\otimes X_3\otimes X_4\otimes Z_3$
$|0000\rangle,|1000\rangle$	$\frac{1}{4}(\alpha|11\rangle-\beta|10\rangle-\gamma|01\rangle+\sigma|00\rangle)$	$X_3\otimes X_4\otimes Z_3\otimes Z_4$
$|0111\rangle,|1111\rangle$	$\frac{1}{4}(-\alpha|11\rangle+\beta|10\rangle-\gamma|01\rangle+\sigma|00\rangle)$	$Z_4\otimes X_3\otimes X_4$

[1] The parentheses in the first column represent what Bob and Charlie might have obtained in a collapsed state after Alice's measurement.

Table 6. Alice, Bob1, Bob2, Charlie2, and Charlie3 perform the measurement and the corresponding unitary operation of Charlie1.

Alice's Measurements	Measurement Results of Bob1 and Bob2	Measurement Results of Charlie2 and Charlie3	Unitary Operation
$\|\Psi^1\rangle(\|\Psi^5\rangle)$	$\|00\rangle,\|10\rangle(\|10\rangle,\|11\rangle)$	$\|++\rangle,\|+-\rangle,\|-+\rangle,\|--\rangle$	$I_3 \otimes I_4$
	$\|10\rangle,\|11\rangle(\|00\rangle,\|10\rangle)$		$Z_3 \otimes I_4$
$\|\Psi^2\rangle(\|\Psi^6\rangle)$	$\|00\rangle,\|10\rangle(\|10\rangle,\|11\rangle)$	$\|++\rangle,\|+-\rangle,\|-+\rangle,\|--\rangle$	$I_3 \otimes Z_4$
	$\|10\rangle,\|11\rangle(\|00\rangle,\|10\rangle)$		$Z_3 \otimes Z_4$
$\|\Psi^3\rangle(\|\Psi^7\rangle)$	$\|00\rangle,\|10\rangle(\|10\rangle,\|11\rangle)$	$\|++\rangle,\|+-\rangle,\|-+\rangle,\|--\rangle$	$I_3 \otimes X_4$
	$\|10\rangle,\|11\rangle(\|00\rangle,\|10\rangle)$		$Z_3 \otimes X_4$
$\|\Psi^4\rangle(\|\Psi^8\rangle)$	$\|00\rangle,\|10\rangle(\|10\rangle,\|11\rangle)$	$\|++\rangle,\|+-\rangle,\|-+\rangle,\|--\rangle$	$Z_3 \otimes Y_4$
	$\|10\rangle,\|11\rangle(\|00\rangle,\|10\rangle)$		$Z_3 \otimes Y_4$
$\|\Psi^9\rangle(\|\Psi^{10}\rangle)$	$\|00\rangle,\|10\rangle$	$\|++\rangle,\|+-\rangle,\|-+\rangle,\|--\rangle$	$X_3 \otimes I_4(Z_4)$
	$\|10\rangle,\|11\rangle$		$Z_3 \otimes X_3 \otimes I_4(Z_4)$
$\|\Psi^{11}\rangle(\|\Psi^{12}\rangle)$	$\|00\rangle,\|10\rangle$	$\|++\rangle,\|+-\rangle,\|-+\rangle,\|--\rangle$	$X_3 \otimes X_4 \otimes I_4(Z_4)$
	$\|10\rangle,\|11\rangle$		$Z_3 \otimes X_3 \otimes X_4 \otimes I_4(Z_4)$
$\|\Psi^{13}\rangle(\|\Psi^{14}\rangle)$	$\|00\rangle,\|10\rangle$	$\|++\rangle,\|+-\rangle,\|-+\rangle,\|--\rangle$	$Y_3 \otimes I_4(Z_4)$
	$\|10\rangle,\|11\rangle$		$Z_3 \otimes Y_3 \otimes I_4(Z_4)$
$\|\Psi^{15}\rangle(\|\Psi^{16}\rangle)$	$\|00\rangle,\|10\rangle$	$\|++\rangle,\|+-\rangle,\|-+\rangle,\|--\rangle$	$Y_3 \otimes X_4(Y_4)$
	$\|10\rangle,\|11\rangle$		$Z_3 \otimes Y_3 \otimes X_4(Y_4)$

4.3. The Hierarchical Quantum Information Splitting Protocol Based on N-Party

In the previous section, we proposed a hierarchical quantum information splitting protocol for a two-qubit state based on an eight-qubit state. In terms of hierarchical quantum information splitting characteristics combined with the ideas proposed in this paper, we can extend this scheme to multi-party communication. In the multi-party protocol, it is assumed that Alice is the sender; Bob1, Bob2, ..., Bobx are high-level communicators, Charlie1, Charle2, ..., Charliey are low-level communicators; and the number of communication participants increases, which means that as the number of channel particles increases, then Alice needs to prepare a multi-qubit state channel. The channel particle is written as

$$\begin{aligned}\left|\phi^N\right\rangle =&\frac{1}{2}[(|0000\rangle+|0101\rangle)(|00\cdots 00\rangle+|00\cdots 11\rangle\\&+|11\cdots 00\rangle+|11\cdots 11\rangle)+(|1010\rangle\\&+|1111\rangle)(|00\cdots 00\rangle-|00\cdots 11\rangle\\&+|11\cdots 00\rangle-|11\cdots 11\rangle)]\end{aligned} \tag{9}$$

Among them, the last half of the multi-qubit state channels, for instance, $|00\ldots 00\rangle$, $|00\ldots 11\rangle, |11\ldots 00\rangle, |11\ldots 11\rangle$, represent the qubits of Charlie1, Charle2, ..., Charliey, respectively; and then we discard the two-qubit owned by the receiver, and the rest are the particles owned by Bob1, Bob2, . . . , Bobx, respectively. Alice still wants to send any two-qubit state, so the system state is

$$
\begin{aligned}
|\zeta\rangle &= |\psi\rangle_{AB} \otimes |\phi^N\rangle = \frac{1}{2}(\alpha|00\rangle + \beta|01\rangle + \gamma|10\rangle \\
&+ \sigma 11\rangle)_{AB} \otimes \frac{1}{2}[(|0000\rangle + |0101\rangle)(|00\ldots00\rangle + |00\ldots11\rangle \\
&+ |11\ldots00\rangle + |11\ldots11\rangle) + (|1010\rangle + |1111\rangle)(|00\ldots00\rangle \\
&- |00\ldots11\rangle + |11\ldots00\rangle - |11\ldots11\rangle)]
\end{aligned}
\tag{10}
$$

We can easily deduce that after Alice conducts the Bell-state measurement of the particle pair (A, 1), (B, 2), the remaining particles will collapse into collapsed states, and the receiver needs to know the information sent by Alice. The other particles and different levels of receivers need further help. When the receiver is a high-level communicator, the measurement results of Charlie1, Charle2, . . . , Charliey—that is, the low-level communicator—can be deduced from each other, so only one person in the low-level communicator ought to perform Z-based single-particle measurement, except the receiver. All high-level communicators must perform single particle measurement and inform the information receiver of the results. Then, the high-level receivers in the communication need to perform relevant unitary operations in order to rebuild the information; when the receivers are low-level communicators, Charlie1, Charle2, . . . , Charliey's results cannot be deduced from each other, then the low-level communicators other than the receiver must perform X-based single-particle measurement on the particles they own, and high-level communicators perform Z-based single-particle measurement on the particles. The receiver is told through the classical channel that after receiving all the results, the receiver conducts the related unitary operation according to the collapsed state.

5. Experiment and Analysis

5.1. Experiments on Hierarchical Quantum Information Splitting Schemes

We used the IBM quantum composer platform to perform the experimental simulation based on the eight-qubit cluster state quantum information separation scheme. The complete process of the experiment is shown in Figure 8, where q0 q7 is the eight-qubit cluster state's quantum channel, q8 and q9 are a two-qubit state, the initial state is $|0\rangle$, the red square is the H gate operation icon, and the symbol with a plus sign is the CNOT gate. The two X connected symbols are the swap gate. I is the preparation process. Firstly, the eight-qubit cluster state was prepared. Since the phase angle of some particle states in the eight-qubit cluster state was $|\phi\rangle_{12345678}$, we used two H gates and one control, a not gate operation, to change their phase. Then, a two-qubit state was prepared. It can be prepared by performing two H gate operations on particle 1 and particle 2. U gate is the parameter gate for constructing any particle, II is the transmission process, Alice performs Bell-state measurement to transmit information, and III is the measurement process. Since the IBM platform cannot provide calculation results for quantum circuit diagrams with more than seven particles, we used the simulator to simulate the results. Obviously, our scheme successfully realized the hierarchical quantum information splitting of any two-qubit state so that the receiver receives the information.

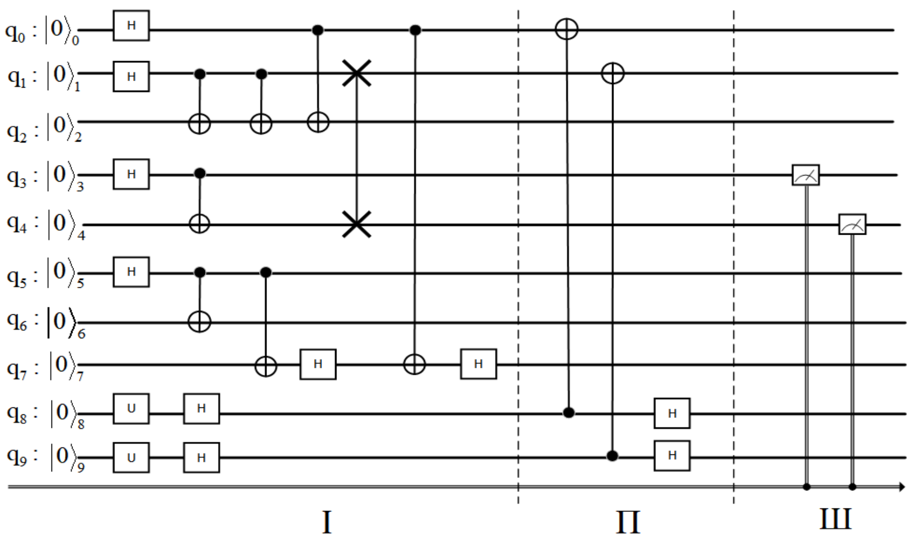

Figure 8. The complete process of the experiment.

For our experimental verification, the theoretical value of the two-qubit state prepared by the IBM platform is $|\phi\rangle_{AB} = \frac{1}{2}(|00\rangle + |01\rangle + |10\rangle + |11\rangle)_{AB}$, and the simulated state $|\phi\rangle_{34} = (\sqrt{0.253}|00\rangle + \sqrt{0.244}|01\rangle + \sqrt{0.258}|10\rangle + \sqrt{0.245}|11\rangle)_{34}$ is calculated according to the actual transmission results in Table 7. Since the formula of quantum fidelity is Equation (11), $\rho = |\phi\rangle_{34}\langle\phi|$, the fidelity of this scheme is about 0.999, indicating that the experimental verification of the hierarchical quantum information splitting scheme based on an eight-qubit cluster state and any two-qubit state is successful.

$$F =_{AB} \langle\phi|\rho|\phi\rangle_{AB} \quad (11)$$

Table 7. Transmission result.

States	Shots	Frequency (%)
$\|00\rangle$	2072	25.3%
$\|01\rangle$	1999	24.4%
$\|10\rangle$	2114	25.8%
$\|11\rangle$	2007	24.5%

5.2. Security Analysis

Generally, quantum attacks include individual attacks and collective attacks. The typical feature of individual attack is to assume that there is an attacker, Eve. Eve tries to use his probe to detect the information of the unknown quantum state, and the collective attack is when the attacker Eve uses multiple probes to detect the quantum state at the same time. Assuming that when the high-level communicator is the receiver, Eve exists and Alice, Bob1, Bob2, Charlie1, Charlie2, and Charlie3 do not know that Eve is trying to eavesdrop on the information, Eve $|\phi\rangle_E = \frac{1}{\sqrt{2}}(|0\rangle + |1\rangle)_E$ successfully entangles his particle on the particle bit of Charlie3. After the particle pair performs the Bell-state measurement, we assume that the measurement result is $|\phi\rangle^+|\phi\rangle^+$, and the collapsed state of the remaining particles is:

$$
\begin{aligned}
|\Psi^1\rangle_{345678E} = &\frac{1}{8}[\alpha(|\psi^0\rangle + |\psi^1\rangle)|0\rangle + \beta(|\psi^2\rangle + |\psi^3\rangle)|0\rangle \\
&+ \gamma(|\psi^4\rangle + |\psi^5\rangle)|0\rangle + \sigma(|\psi^6\rangle + |\psi^7\rangle)|0\rangle \\
&+ \alpha(|\psi^0\rangle + |\psi^1\rangle)|1\rangle + \beta(|\psi^2\rangle + |\psi^3\rangle)|1\rangle \\
&+ \gamma(|\psi^4\rangle + |\psi^5\rangle)|1\rangle + \sigma(|\psi^6\rangle + |\psi^7\rangle)|1\rangle]_{345678E} \\
= &\frac{1}{8\sqrt{2}}[(\alpha|00\rangle + \beta|01\rangle + \gamma|10\rangle + \sigma|11\rangle)|0\rangle|0000\rangle \\
&+ (\alpha|00\rangle + \beta|01\rangle + \gamma|10\rangle + \sigma|11\rangle)|0\rangle|0001\rangle \\
&+ (\alpha|00\rangle + \beta|01\rangle - \gamma|10\rangle - \sigma|11\rangle)|0\rangle|1110\rangle \\
&+ (\alpha|00\rangle + \beta|01\rangle - \gamma|10\rangle - \sigma|11\rangle)|0\rangle|1111\rangle \\
&+ (\alpha|00\rangle + \beta|01\rangle + \gamma|10\rangle + \sigma|11\rangle)|1\rangle|0000\rangle \\
&+ (\alpha|00\rangle + \beta|01\rangle + \gamma|10\rangle + \sigma|11\rangle)|1\rangle|0001\rangle \\
&+ (\alpha|00\rangle + \beta|01\rangle - \gamma|10\rangle - \sigma|11\rangle)|1\rangle|1110\rangle \\
&+ (\alpha|00\rangle + \beta|01\rangle - \gamma|10\rangle - \sigma|11\rangle)|1\rangle|1111\rangle]_{345678E}
\end{aligned} \tag{12}
$$

Next, Bob1 needs the help of other communicators. After Bob2 and Charlie1 perform single particle measurement, the state will collapse again. Assuming that the results of Bob2 and Charlie1 are both $|0\rangle$, as in Equation (13), due to Eve's attack, there is no change in the quantum state. We can infer that Eve has not detected any message, and the scheme is safe. Similarly, when Eve entangles multiple particle bits, $|\phi\rangle_E$ will not change, and the collective attack is invalid.

$$
|\phi\rangle_{34E} = \frac{1}{4}(\alpha|00\rangle + \beta|01\rangle + \gamma|10\rangle + \sigma|11\rangle)_{34} \otimes \frac{1}{\sqrt{2}}(|0\rangle + |1\rangle)_E \tag{13}
$$

In addition to this, there is also a man-in-the-middle attack, in which the attacker, Eve, pretends to be a member of the communication team, tries to intercept the conversation in the communication, and after intercepting the message, sends the message he prepared to the receiver and convinces him that it is a message to be sent to him by a participant in the communication. However, since the receiver ought to perform the relevant unitary operation according to the received measurement result to restore the original information, the message sent by Eve is a fake message, which is not in the result, so the receiver cannot find the corresponding response according to Eve's message. The operation performed cannot reconstruct any two-particle state, so the communication is found to be abnormal and terminated. To sum up, none of these attacks can be effective in the scheme we designed, and the eavesdropper cannot eavesdrop on the information, which shows that the scheme can resist the attack and has strong security.

5.3. Scheme Comparison Analysis

To further demonstrate that our scheme (OS) is efficient, we compare this scheme with those in [7,19,21,22]. We compare them with the four aspects of quantum resource consumption (QS), quantum bits transmitted (QT), transmission efficiency, and the number of communication participants (NC). Quantum resource consumption refers to the number of particles in the quantum channel used, the number of qubits transmitted is the number of particles that the scheme can transmit, and the transmission efficiency is calculated based on the number of quanta transmitted and the number of channel particles used to transmit these quantum states. The calculation formula for transmission efficiency is as follows:

$$
\eta = \frac{c}{q+t} \tag{14}
$$

where c is the number of qubits transmitted, q is the number of bits used by the quantum channel, and t is the number of classical bits, which is the number of bits transmitted through the classical channel. According to Equation (14), the number of particles transmitted in reference [19] is one, and the transmission efficiency is $\eta_1 = \frac{1}{4+4} = \frac{1}{8}$ using the four-qubit entangled state as the quantum channel. Three schemes are listed in reference [7]. According to its protocol rules, we conclude that when the number of communication participants is five, the number of channel particles used is ten. The transmitted quantum state is any two-qubit state, and then the transmission efficiency is $\eta_1 = \frac{2}{10+10} = \frac{1}{10}$. Similarly, the transmission efficiency of other schemes can be calculated, and the results are evinced in Table 8.

Table 8. Resampling error value vs. cross validation error value.

Schemes	QS	QT	Transmission Efficiency (%)	NC
Ref. [7]	10	2	10%	5
Ref. [19]	4	1	12.5%	4
Ref. [21]	4	1	12.5%	4
Ref. [22]	8	2	12.5%	4
OS	8	2	14.5%	5

In addition to the above four aspects, other schemes have never used machine learning to solve the specific allocation problem of channel particles. We combined machine learning with quantum communication. After data preprocessing, we comprehensively evaluated the decision tree algorithm's prediction model and allocated quantum resources for communication according to the determined scheme. Moreover, this scheme takes many operations, especially when preparing the quantum channel; the various gate operations taken make the quantum state change more complicated. It is safer when transmitting the particle state. The scheme does not need to perform operations like those in [21] and the POVM measurements in reference [22], which can utilize limited quantum resources to enable more communicators to participate in communication, so our scheme has the characteristics of high efficiency and low consumption of quantum resources.

6. Discussion

The results of this article prove that quantum communication can be effectively combined with a machine learning algorithms, and the latter can improve the efficiency of quantum communication, which will bring great benefit to the practical application of quantum communication. In the future, we will continue to study the effective combination of quantum communication and machine learning to take quantum communication from theory to reality as soon as possible.

7. Conclusions

This paper proposed a two-qubit hierarchical quantum information splitting scheme using eight particle states as quantum channels and extends it to multi-particle states. In the early stage, we introduced the decision tree algorithm of machine learning into quantum communication and proved by experiments that the decision tree algorithm can determine the optimal allocation strategy, and then formulated the corresponding hierarchical quantum information splitting scheme according to this strategy. Assuming Alice is the sender, Bob1, Bob2, Charlie1, Charlie2, and Charlie3 are divided into high-level and low-level communicators. Alice selects one of them to communicate. After Alice performs Bell-state measurement on particle pairs, different receivers need different communicators to perform single-particle measurement and tell the results to the receiver through the classical channel. The receiver can perform the unitary operation to reconstruct a two-qubit state according to the corresponding results. Compared with the previous hierarchical quantum information splitting scheme [7,19,21,22], our advantage is to design the scheme according to the decision, which makes the scheme more effective in practical applications and can transmit more particle information with fewer particles. We also carried out experimental verification, security analysis, and comparative analysis of the scheme, showing that the scheme has high security and reliability. We will continue researching cross-quantum informatics and quantum physics with more disciplines in future work. This part of the theoretical research content and experiment will also become more and more mature.

Author Contributions: Conceptualization, D.L., Y.Z. and M.L.; methodology, D.L. and Y.Z.; software, Y.Z.; validation, D.L. and Y.Z.; formal analysis, J.Z.; investigation, X.L., X.Y.; resources, D.L.; data curation, Y.Z., J.Z. and Y.T.; writing—original draft preparation, Y.Z.; writing—review and editing, D.L., Y.Z., J.Z., Y.T. and X.Y.; supervision, D.L. and M.L. All authors have read and agreed to the published version of the manuscript.

Funding: This work was supported in part by the National Natural Science Foundation of China (62172060), Key R&D Project of Sichuan Province Science and Technology Plan (2020YFS0445), Sichuan Science and Technology Program (2022YFG0316).

Data Availability Statement: Not applicable.

Acknowledgments: Thank you to the editor reviewers for reviewing this article in their busy schedules, and thank the teachers for their careful guidance and help.

Conflicts of Interest: The authors declare no conflict of interest.

References

1. Hillery, M.; Buzek, V. Secret sharing via quantum entanglement. *Acta Phys. Slovaca* **1999**, *49*, 533–540.
2. Murao, M.; Jonathan, D.; Plenio, M.; Vedral, V. Quantum telecloning and multiparticle entanglement. *Phys. Rev.* **1999**, *59*, 156. [CrossRef]
3. Grudka, A.; Wójcik, A. Multiparty d-dimensional quantum information splitting. *arXiv* **2002**, arXiv:quant-ph/0205111.
4. Brádler, K.; Dušek, M. Secret-message sharing via direct transmission. *J. Opt. Quantum Semiclassical Opt.* **2003**, *6*, 63. [CrossRef]
5. Xu, G.; Wang, C.; Yang, Y.X. Hierarchical quantum information splitting of an arbitrary two-qubit state via the cluster state. *Quantum Inf. Process.* **2014**, *13*, 43–57. [CrossRef]
6. Panigrahi, P.K.; Karumanchi, S.; Muralidharan, S. Minimal classical communication and measurement complexity for quantum information splitting of a two-qubit state. *Pramana* **2009**, *73*, 499–504. [CrossRef]
7. Zhang, W.; Liu, Y.m.; Zhang, Z.j.; Cheung, C.Y. Splitting a qudit state via Greenberger–Horne–Zeilinger states of qubits. *Opt. Commun.* **2010**, *283*, 628–632. [CrossRef]
8. Bai, M.Q.; Mo, Z.W. Hierarchical quantum information splitting with eight-qubit cluster states. *Quantum Inf. Process.* **2013**, *12*, 1053–1064. [CrossRef]
9. Shukla, C.; Pathak, A. Hierarchical quantum communication. *Phys. Lett.* **2013**, *377*, 1337–1344. [CrossRef]
10. Ma, P.C.; Chen, G.B.; Li, X.W.; Zhan, Y.B. Hierarchical controlled remote state preparation by using a four-qubit cluster state. *Int. J. Theor. Phys.* **2018**, *57*, 1748–1755. [CrossRef]
11. Zha, X.W.; Miao, N.; Wang, H.F. Hierarchical quantum information splitting of an arbitrary two-qubit using a single quantum resource. *Int. J. Theor. Phys.* **2019**, *58*, 2428–2434. [CrossRef]
12. Wang, X.W.; Zhang, D.Y.; Tang, S.Q.; Zhan, X.G.; You, K.M. Hierarchical quantum information splitting with six-photon cluster states. *Int. J. Theor. Phys.* **2010**, *49*, 2691–2697. [CrossRef]
13. Zhang, Q.Y.; Zhan, Y.B. Quantum information splitting by using asymmetric multi-particle state. *Int. J. Theor. Phys.* **2012**, *51*, 3037–3044. [CrossRef]
14. Xu, G.; Shan, R.T.; Chen, X.B.; Dong, M.; Chen, Y.L. Probabilistic and hierarchical quantum information splitting based on the non-maximally entangled cluster state. *Cmc-Comput. Mater. Contin.* **2021**, *69*, 339–349. [CrossRef]
15. Guo, W.M.; Qin, L.R. Hierarchical and probabilistic quantum information splitting of an arbitrary two-qubit state via two cluster states. *Chin. Phys. B* **2018**, *27*, 110302. [CrossRef]
16. Li, S.W.; Jiang, M.; Jiang, F.; Chen, X.P. Multi-qudit information splitting with multiple controllers. *Quantum Inf. Process.* **2014**, *13*, 1057–1066. [CrossRef]
17. Huang, G.Q.; Luo, C.L. Splitting Quantum Information with Five-Atom Cluster State in Cavity QED. *Int. J. Theor. Phys.* **2011**, *50*, 401–406. [CrossRef]
18. Li, Y.h.; Li, X.l.; Sang, M.h.; Nie, Y.y. Splitting unknown two-qubit state using five-qubit entangled state. *Int. J. Theor. Phys.* **2014**, *53*, 111–115. [CrossRef]
19. Jouguet, P.; Kunz-Jacques, S.; Leverrier, A.; Grangier, P.; Diamanti, E. Experimental demonstration of long-distance continuous-variable quantum key distribution. *Nat. Photonics* **2013**, *7*, 378–381. [CrossRef]

20. Boaron, A.; Boso, G.; Rusca, D.; Vulliez, C.; Autebert, C.; Caloz, M.; Perrenoud, M.; Gras, G.; Bussières, F.; Li, M.J.; et al. Secure quantum key distribution over 421 km of optical fiber. *Phys. Rev. Lett.* **2018**, *121*, 190502. [CrossRef]
21. Yin-Ju, L. A novel practical quantum secure direct communication protocol. *Int. J. Theor. Phys.* **2021**, *60*, 1159–1163. [CrossRef]
22. Zhang, Y.Q.; Yang, L.J.; He, Q.L.; Chen, L. Machine learning on quantifying quantum steerability. *Quantum Inf. Process.* **2020**, *19*, 263. [CrossRef]
23. Wallnöfer, J.; Melnikov, A.A.; Dür, W.; Briegel, H.J. Machine learning for long-distance quantum communication. *PRX Quantum* **2020**, *1*, 010301. [CrossRef]
24. Lamata, L. Quantum reinforcement learning with quantum photonics. *Photonics* **2021**, *8*, 33. [CrossRef]
25. Al-Mohammed, H.A.; Al-Ali, A.; Yaacoub, E.; Qidwai, U.; Abualsaud, K.; Rzewuski, S.; Flizikowski, A. Machine Learning Techniques for Detecting Attackers During Quantum Key Distribution in IoT Networks With Application to Railway Scenarios. *IEEE Access* **2021**, *9*, 136994–137004. [CrossRef]
26. Ren, Z.A.; Chen, Y.P.; Liu, J.Y.; Ding, H.J.; Wang, Q. Implementation of machine learning in quantum key distributions. *IEEE Commun. Lett.* **2020**, *25*, 940–944. [CrossRef]
27. Bebrov, G.; Dimova, R. Efficient quantum secure direct communication protocol based on Quantum Channel compression. *Int. J. Theor. Phys.* **2020**, *59*, 426–435. [CrossRef]
28. Verma, V. Bidirectional quantum teleportation by using two GHZ-states as the quantum channel. *IEEE Commun. Lett.* **2020**, *25*, 936–939. [CrossRef]
29. Feng, Z.J.; Tang, L.; Xiang, Y.; Mo, Z.W.; Bai, M.Q. Authenticated quantum dialogue protocol based on four-particle entangled states. *Mod. Phys. Lett.* **2021**, *36*, 2150189. [CrossRef]
30. Choudhury, B.S.; Samanta, S. A Controlled Asymmetric Quantum Conference. *Int. J. Theor. Phys.* **2022**, *61*, 14. [CrossRef]
31. Wang, P.; Yan, Z.; Han, G.; Yang, H.; Zhao, Y.; Lin, C.; Wang, N.; Zhang, Q. A2E2: Aerial-assisted energy-efficient edge sensing in intelligent public transportation systems. *J. Syst. Archit.* **2022**, *129*, 102617. [CrossRef]
32. Liang, J.; Qin, Z.; Xiao, S.; Ou, L.; Lin, X. Efficient and secure decision tree classification for cloud-assisted online diagnosis services. *IEEE Trans. Dependable Secur. Comput.* **2019**, *18*, 1632–1644. [CrossRef]
33. Yan, X.; Cui, B.; Xu, Y.; Shi, P.; Wang, Z. A method of information protection for collaborative deep learning under GAN model attack. *IEEE/ACM Trans. Comput. Biol. Bioinform.* **2019**, *18*, 871–881. [CrossRef] [PubMed]
34. Kamiński, B.; Jakubczyk, M.; Szufel, P. A framework for sensitivity analysis of decision trees. *Cent. Eur. J. Oper. Res.* **2018**, *26*, 135–159. [CrossRef]
35. Wang, P.; Zhao, Y.; Obaidat, M.S.; Wei, Z.; Qi, H.; Lin, C.; Xiao, Y.; Zhang, Q. Blockchain-Enhanced Federated Learning Market with Social Internet of Things. *IEEE J. Sel. Areas Commun.* **2022**. [CrossRef]
36. Wang, P.; Pan, Y.; Lin, C.; Qi, H.; Ren, J.; Wang, N.; Yu, Z.; Zhou, D.; Zhang, Q. Graph Optimized Data Offloading for Crowd-AI Hybrid Urban Tracking in Intelligent Transportation Systems. *IEEE Trans. Intell. Transp. Syst.* **2022**. [CrossRef]